



Originally published as:

Shen, B., Stephansson, O., Rinne, M., Amemiya, K., Yamashi, R., Toguri, S., Asano, H. (2011): FRACOD modeling of rock fracturing and permeability change in excavation-damaged zones. - International Journal of Geomechanics, 11, 4, 302-313

DOI: 10.1061/(ASCE)GM.1943-5622.0000034

FRACOD Modeling of Rock Fracturing and Permeability Change in Excavation-Damaged Zones

B. Shen¹; O. Stephansson²; M. Rinne³; K. Amemiya⁴; R. Yamashi⁵; S. Toguri⁶; and H. Asano⁷

Abstract: The characterization of the excavation-damaged zone (EDZ) around an underground excavation is a major research topic for deep geological disposal of medium- to high-level radioactive waste. Rock fracturing because of excavation and thermal loading and its resultant rock mass permeability change in the EDZ are important for the construction project and long-term safety. A new function to predict rock mass permeability change in fractured rocks has been developed and added to the existing fracture mechanics code FRACOD. The new functions in FRACOD have been applied to predict the extent of EDZ and permeability change in the vicinity of the tunnel sealing experiment (TSX) tunnel of the Underground Research Laboratory (Canada), the zone of excavation disturbance experiments (ZEDEX) tunnel of the Äspö Hard Rock Laboratory (Sweden), and the deposition tunnels in crystalline and sedimentary rocks (Japan). The predicted EDZ and its permeability are consistent with the measurement data of the TSX tunnel and ZEDEX tunnel. The results from both tests indicate that FRACOD with the new function is capable of realistically predicting the EDZ and permeability change.

DOI: 10.1061/(ASCE)GM.1943-5622.0000034.

CE Database subject headings: Rock mechanics; Cracking; Excavation; Damage; Permeability; Validation.

Author keywords: Rock fracture mechanics; Excavation-damaged zone (EDZ); Permeability; Validation.

Introduction

Whenever rock is excavated, the zone around the excavation is altered. Two different types of alteration zones are possible: (1) an excavation-damaged zone, and (2) an excavation-disturbed zone. The excavation-damaged zone (EDZ) is defined as the part of the rock mass adjacent to an opening where irreversible deformation and fracture propagation and/or new fractures are developed. The excavation disturbed zone (EdZ) is defined as the zone beyond the EDZ where stress redistribution occurs, but the deformations are mainly elastic and reversible with minor changes in permeability. A review of EDZ and EdZ in different rock types is presented by Tsang *et al.* (2005). This article examines the EDZ. There

are principal four factors that affect the characteristics and extent of the EDZ: (1) excavation method; (2) the in situ stress and its orientation; (3) strength and deformability of the rock mass; and (4) hydraulic pressure in the groundwater surrounding the opening. When an underground opening is excavated, the virgin stress in the rock mass will be changed, and a stress concentration and reduction will appear at the periphery of the opening, which might lead to rock fall and spalling. The excavation method used will cause an additional EDZ, and its extent depends on the excavation method. Drilling and blasting generally cause greater damage than tunnel-boring machines (TBMs). The zone of excavation disturbance experiments (ZEDEX) tunnel in the Äspö Hard Rock Laboratory compared the extent of EDZ in tunneling caused by TBMs and drilling and blasting (Emsley *et al.* 1997).

Certain rock features, such as porosity, microstructures, and hydraulic conductivity in the EDZ around deposition tunnels, affect the long-term safety aspects. Therefore, it is of the utmost importance to minimize the extent of EDZ and to understand its evolution with time. The EDZ can be reduced by orienting the excavations and tunnels so that the longest axes of the openings coincide with the orientation of the maximum principal stress, optimizing the geometry of the openings to avoid stress concentrations, and avoiding areas with low rock strength.

The rock fracture mechanics program FRACOD has been used in this study. FRACOD was designed to simulate fracture initiation, propagation, and coalescence in hard rocks (Shen and Stephansson 1994; Shen 2002), and it has been used in a number of research projects for the Swedish nuclear waste deposition, including the Äspö pillar stability experi-

¹ CSIRO Exploration and Mining, Qld 4069, Brisbane, Australia.

² GFZ German Research Centre for Geosciences, D-14473 Potsdam, Germany (corresponding writer). E-mail: ove@stephansson.de

³ FRACOM Ltd., Farfarsbacken 14, FIN-02400 Kyrklätt, Finland.

⁴ Hazama Corporation, Nuclear Power Dept., 2-2-5 Toranomon Minatoku, Tokyo, Japan.

⁵ Hazama Corporation, Nuclear Power Dept., 2-2-5 Toranomon Minatoku, Tokyo, Japan.

⁶ RWMC Radioactive Waste Management Funding and Research Center, EBS Technology Research Project, 1-15-7 Tsukishima Chuo-ku, Tokyo, Japan.

⁷ RWMC Radioactive Waste Management Funding and Research Center, EBS Technology Research Project, 1-15-7 Tsukishima Chuo-ku, Tokyo, Japan.

Note. This manuscript was submitted on September 2, 2009; approved on April 7, 2010; published online on April 10, 2010. Discussion period open until January 1, 2012; separate discussions must be submitted for individual papers. This paper is part of the International Journal of Geomechanics, Vol. 11, No. 4, August 1, 2011.

ment (APSE) (Rinne *et al.* 2002, 2003a). It has also been used in modeling borehole breakouts (Shen *et al.* 2002). The code has the capacity to predict fracture initiation, propagation, and coalescence of preexisting joints and newly formed fractures in the vicinity of excavations. It also predicts the locations and relative magnitude of acoustic emission (AE) or microseismicity.

This article concerns the latest version of FRACOD, in which the theoretical formulations and the numerical procedures of a new permeability function are described, together with the following validations and applications:

- Validation tests of FRACOD against the Atomic Energy of Canada Limited (AECL) Underground Research Laboratory (URL) permeability measurement results in the tunnel sealing experiment (TSX) tunnel in Canada.
- Validation tests against the ZEDEX measurement results in the drill and blast tunnel and the TBM tunnel of the Äspö Hard Rock Laboratory, Sweden.
- Application of FRACOD to predict EDZ permeability of the Japanese deposition tunnel in crystalline fractured rock.

Hydraulic Conductivity in Fractured Rock Mass

A fractured rock mass consists of the intact rock and rock fractures. Fluid flow in a fractured rock mass occurs in both the fractures and through the porous intact rock, although often the fracture flow is dominant. The hydraulic conductivity of a fractured rock mass is a combination of that of the fractures and the intact rock. Depending on the distribution of the fractures, the equivalent rock mass conductivity may or may not be easily obtained.

Rock Mass with a Single Fracture

Fig. 1 shows a rock mass with a through-going fracture. For a two-dimensional (2D) problem, the total flow volume in the intact rock and the fractures with aperture a can be written as

Fracture

$$Q_f = \frac{a^3}{12\mu} \frac{dp}{dl} \quad (1)$$

Intact rock

$$Q_r = wK_r \frac{dp}{dl} \quad (2)$$

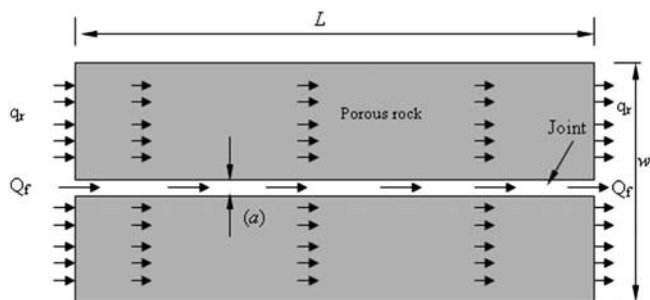


Figure 2. Idealized hydraulic model of a fractured rock mass

For the whole fractured rock mass, the total flow volume is

$$Q = Q_f + Q_r = -w \left(\frac{a^3}{12\mu w} + K_r \right) \frac{dp}{dl} \quad (3)$$

or

$$Q = -w(K_f + K_r) \frac{dp}{dl} = wK \frac{dp}{dl} \quad (4)$$

where K = total conductivity of rock mass; K_f = conductivity of fracture; K_r = conductivity of intact rock; and w = width of rock mass element.

In Eq. (4), the fracture conductivity is expressed as

$$K_f = \frac{a^3}{12\mu w} \quad (5)$$

and the total rock mass conductivity is expressed as

$$K = K_f + K_r \quad (6)$$

The fracture conductivity in the equivalent form of the porous rock conductivity is expressed as a function of the fracture aperture (a) and the width of rock mass element (w). In a rock mass that has a set of fractures, the width of the rock mass element (w) is actually the fracture spacing.

Rock Mass with Multiple Subparallel Fractures

A case of a rock mass with three subparallel fractures is illustrated in Fig. 2. The fluid pressure loss in each fracture is the same, whereas the total flow volume of all fractures is the sum of that of each individual fracture.

The total flow volume is then calculated by

$$\begin{aligned} Q &= Q_f^{(1)} + Q_f^{(2)} + Q_f^{(3)} + Q_r \\ &= -K_f^{(1)} \frac{\Delta p}{L/\cos\theta_1} - K_f^{(2)} \frac{\Delta p}{L/\cos\theta_2} \\ &\quad - K_f^{(3)} \frac{\Delta p}{L/\cos\theta_3} - K_r \frac{\Delta p}{L} \end{aligned} \quad (7)$$

The total rock mass conductivity in this case is a simple sum of those of all the fractures and the intact rock:

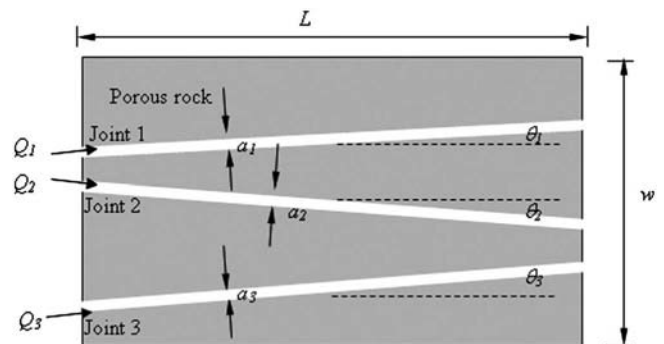


Figure 1. Rock mass with multiple subparallel fractures

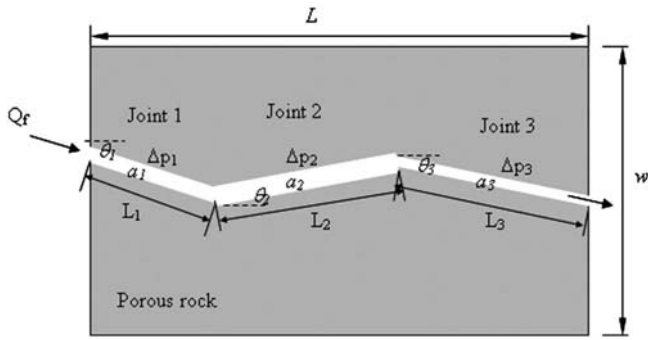


Figure 3. Rock mass with multiple connected fractures

$$K = K_f^{(1)} \cos \theta_1 + K_f^{(2)} \cos \theta_2 + K_f^{(3)} \cos \theta_3 + K_r \quad (8)$$

or

$$K = \frac{a_1^3 \cos \theta_1 + a_2^3 \cos \theta_2 + a_3^3 \cos \theta_3}{12\mu w} + K_r \quad (9)$$

where a_1 , a_2 , and a_3 = aperture of the three parallel fractures.

If there are n parallel fractures, Eq. (9) can be rewritten as

$$K = \frac{\sum_{i=1,n} a_i^3 \cos \theta_i}{12\mu w} + K_r \quad (10)$$

Rock Mass with a Serial of Connected Fractures

A case of a rock mass with three connected fractures is illustrated in Fig. 3. The total fracture conductivity must be analyzed by using that of each individual fracture.

The flow volume in each fracture is the same, whereas the total pressure loss is the sum of that of individual fractures. Thus

$$Q_f = -K_f \frac{\Delta p}{L} = -K_f \frac{\Delta p_1 + \Delta p_2 + \Delta p_3}{L_1 \cos \theta_1 + L_2 \cos \theta_2 + L_3 \cos \theta_3} \quad (11)$$

where the pressure loss in each fracture can be calculated using the equations

$$\begin{aligned} \Delta p_1 &= \frac{L_1 Q_f}{K_f^{(1)}} \\ \Delta p_2 &= \frac{L_2 Q_f}{K_f^{(2)}} \\ \Delta p_3 &= \frac{L_3 Q_f}{K_f^{(3)}} \end{aligned} \quad (12)$$

Substituting the pressure loss in Eq. (11) by the expressions in Eq. (12) results in

$$Q_f = K_f \frac{\frac{L_1 Q_f}{K_f^{(1)}} + \frac{L_2 Q_f}{K_f^{(2)}} + \frac{L_3 Q_f}{K_f^{(3)}}}{L_1 \cos \theta_1 + L_2 \cos \theta_2 + L_3 \cos \theta_3} \quad (13)$$

Eq. (13) can be simplified to obtain the expression for K_f :

$$K_f = \frac{L_1 \cos \theta_1 + L_2 \cos \theta_2 + L_3 \cos \theta_3}{L_1/K_f^{(1)} + L_2/K_f^{(2)} + L_3/K_f^{(3)}} \quad (14)$$

The total fracture conductivity is dominated by the least conductive fracture. In the extreme case, if one of the three fractures is impermeable (zero conductivity), the whole fracture flow path will be blocked, and the resultant fracture conductivity will be zero.

Considering the general case with n connected fractures and taking into account the rock conductivity, the total rock mass conductivity can be calculated by

$$K = \frac{\sum_{i=1,n} L_i \cos \theta_i}{\sum_{i=1,n} L_i / K_f^{(i)}} \quad (15)$$

where

$$K_f^{(i)} = \frac{a_i^3}{12\mu w}$$

Rock Mass with Several Fractures

In a rock mass with subparallel fractures, the fluid pressure loss in each fracture is the same, whereas the total flow volume of all fractures is the sum of that of each individual fracture. If there are n parallel fractures with a dip angle θ to the horizontal direction, the total rock mass conductivity can be calculated by Eq. (10).

In a rock mass with a serial of n connected fractures, the total rock mass conductivity is governed by a summation of the contribution from each individual fracture, as shown in Eq. (15).

For a rock mass with randomly distributed fractures, it is very difficult to obtain an analytical expression for the overall permeability. An approximation method is used in this study to estimate the overall rock mass conductivity. Two extreme cases are considered. The first is that all the fractures are linked end-to-end in a serial pattern. The overall hydraulic conductivity of all the fractures in this pattern is given by the first term of the right side of Eq. (15). It is often dominated by the least-conductive fractures, hence it represents the lower end of the possible conductivity values.

The second case is that all fractures are overlapped in a parallel pattern. Then the overall hydraulic conductivity of all the fractures in this pattern is given by the first term in Eq. (10). It is often dominated by the maximum conductivity of all the fractures, hence it represents the higher end of the possible conductivity values.

The overall fracture conductivity is estimated by using the mathematical mean value of its higher- and lower-end values, as follows:

$$K_f = \left[\frac{\sum_{i=1,n} L_i K_f^{(i)} \cos \theta_i}{\sum_{i=1,n} L_i / K_f^{(i)}} \right] \quad (16)$$

Using Eq. (16), the fracture system is simplified to a single

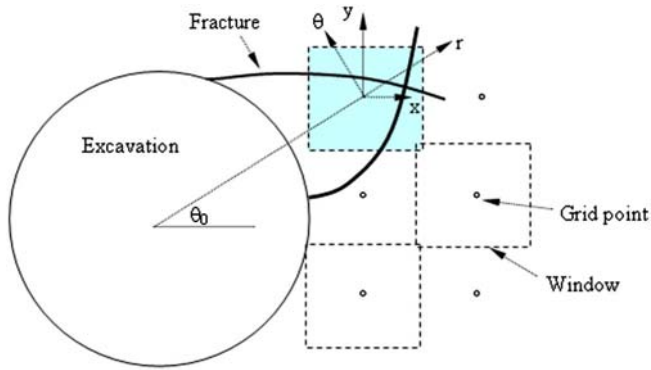


Figure 4. Grid points and windows used for conductivity estimation

equivalent fracture with a conductivity K_f . The effective length of the equivalent fracture is estimated by

$$L_f = \sum_{i=1,n} L_i \cos \theta_i \quad (17)$$

The effective length L_f may be longer or shorter than the rock mass element L . If it is shorter than L , the equivalent fracture is contained in the rock mass. The conductivity of the rock mass system is then estimated by

$$K = (K_f + K_r)^{L_f/L} (K_r)^{(L-L_f)/L} \quad (18)$$

In Eq. (18), if the equivalent length L_f is zero (i.e., no frac-

tures), the resultant rock mass conductivity is the intact rock conductivity K_r only. If L_f equals L , the resultant rock mass conductivity will be $K_f + K_r$.

If the equivalent fracture length L_f is greater than L , it will be treated as one (or more) through-going fracture with length of L and a contained fracture with a length of $L'_f = L_f - L$. Then the conductivity of rock mass is estimated by

$$K = \text{integer} \left(\frac{L_f}{L} \right) \cdot K_f + (K_f + K_r)^{L'_f/L} (K_r)^{(L-L'_f)/L} \quad (19)$$

Predicting Conductivity using FRACOD

FRACOD simulates rock mass failure using an explicit fracturing process, such as fracture initiation, propagation, and coalescence. The normal and shear displacements of the existing and new fractures are predicted and recorded during the failure process. It predicts the fracture aperture change by using the normal displacement of the fractures. Each fracture is discretized into a number of displacement discontinuity (DD) elements in a FRACOD model. Each element has a constant fracture aperture calculated on the basis of its normal displacement. The conductivity of each fracture element is calculated in FRACOD by

$$K_f = \frac{a^3 g \rho}{12 \mu w} \quad (\text{m/s}) \quad (20)$$

where μ = dynamic viscosity (for water at room temperature,

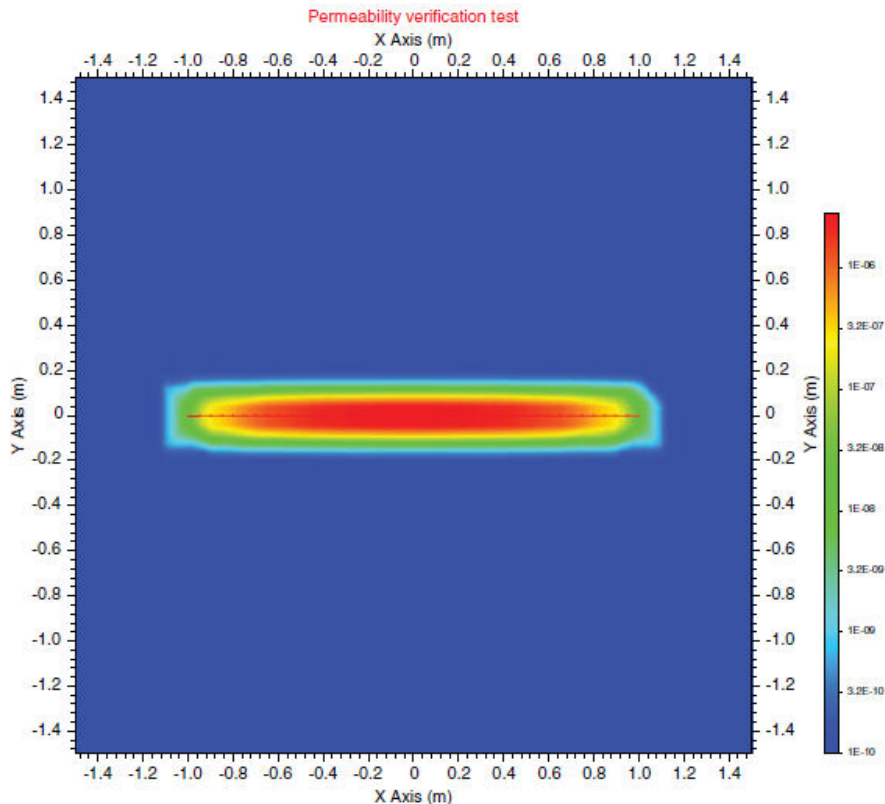


Figure 5. (Color) Predicted hydraulic conductivity of a simple test problem

$\mu = 1.0 \times 10^3$ Pa s); w = width of the fracture zone, or gridpoint spacing used for estimation (m); ρ = water density (kg/m^3); and g = acceleration of gravity (m/s^2).

In FRACOD models, a number of grid points are specified in the solid, and the stresses and displacements are calculated at each grid point. These grid points are also used to estimate the rock mass conductivity. As shown in Fig. 4, a square window was specified around each grid point for the conductivity calculation. Only the fracture elements within the defined window are considered.

For a rock mass with explicit fractures, the hydraulic conductivity is direction-dependent. Therefore, each grid point must consider at least two orthogonal directions (i.e., x and y). For problems with circular excavations, the radial and tangential directions must also be considered (see Fig. 4).

The rock mass conductivity in the x -direction (K_x) can be estimated by using Eqs. (16)-(19), and θ_i in these equations is the angle of each fracture element to the x -axis. The rock mass conductivity in the y -direction (K_y) is calculated by replacing $\cos \theta_i$ with $\sin \theta_i$ in the same equations.

Several tests have been performed using the new hydraulic conductivity function in FRACOD. A simple model with a single fracture is modeled. The fracture is contained in a large rock mass and subjected to uniaxial tension. The key mechanical properties of the rock and the fractures are listed below:

- In situ stresses: $\sigma_x = 0$ MPa; $\sigma_y = 1$ MPa; $\sigma_{xy} = 0$
- Rock mass: Poisson's ratio $\nu = 0.25$; Young's modulus $E = 40$ GPa
- Fracture: Initial aperture $a_0 = 1 \times 10^{-6}$ m; residual aperture $a_r = 1 \times 10^{-6}$ m; half-fracture length $l = 1$ m; element size = 0.05 m
- Grind point window size: 0.25 m
- Intact rock conductivity: $K_r = 1 \times 10^{-10}$ m/s

The theoretical fracture opening displacement is calculated by

$$d_n(x) = \frac{4(1 - \nu^2)}{E} \sigma_y l \sqrt{(1 - x^2/l^2)} \quad (21)$$

The maximum opening at the crack center is calculated by

$$d_n(x=0) = \frac{4(1 - \nu^2)}{E} \sigma_y l \sqrt{(1 - x^2/l^2)} \quad (22)$$

$$= \frac{4 \times (1 - 0.25^2)}{40,000} \times 1.0 = 9.375 \times 10^{-5} \text{ m}$$

The maximum aperture a at the crack center is 9.375×10^{-6} m. The fracture hydraulic conductivity at the center point is

$$K_f = \frac{a^3 g \rho}{12 \mu w} = \frac{(9.375 \times 10^{-5})^3 \times 9.81 \times 1,000}{12 \times 1.0 \times 10^{-3} \times 0.25} = 2.7 \times 10^{-6} \text{ m/s}$$

For a rock mass element with a width of 0.25 m, the total equivalent rock mass conductivity at the crack center is calculated by

$$K = K_r + K_f = 2.7 \times 10^{-6} \text{ m/s}$$

In this case, the intact rock conductivity is much smaller than that of the fractures, and it has an insignificant contribution to the overall conductivity.

The numerically predicted conductivity distribution around the crack is shown in Fig. 5. The predicted maximum conductivity is 2.83×10^{-6} m/s. It agrees fairly well with the analytical solution. The numerical error is within 5%.

Table 1. Input Parameters for the AECL's URL Validation Study

Input parameter	Value	Source
Rock type	Lac du Bonnet granite	Hajiabdolmajid (2002); Souley et al. (2001)
Intact compressive strength (σ_c)	224 MPa	Hajiabdolmajid (2002)
Intact tensile strength (σ_t)	10 MPa	
Rock mass strength (σ_{cm})	128 MPa	
Internal friction angle (φ)	48°	
Intact rock cohesion (c)	3 MPa	based on σ_c and φ
Young's modulus (E)	60 GPa	Hajiabdolmajid (2002)
Poisson's ratio (ν)	0.2	
Fracture toughness K_{Ic}	0.96 MPa m ^{1/2}	Souley et al. (2001)
Fracture toughness K_{IIc}	2 MPa m ^{1/2}	Assumed
In situ stress σ_1	-55 MPa	Souley et al. (2001)
In situ stress σ_2	-48 MPa	
In situ stress σ_3	-12.8 MPa	
Fracture initiation level (σ_{ci}):	0.3 σ_c or 67 MPa	Emsley et al. (1997)
Fracture normal stiffness (K_n)	13,800 GPa/m	Assumed
Fracture normal stiffness (K_s)	3,099 GPa/m	
Fracture friction angle (φ)	48°	From intact rock strength
Fracture cohesion (c)	43 MPa	
Fracture dilation angle (φ_d)	5°	Assumed
In-situ hydraulic conductivity (K_{is})	1.5×10^{-14} m/s	Souley et al. (2001)
Fracture initial aperture (e_{initial})	10×10^{-6} m	Assumed
Fracture residual aperture ($e_{\text{residual}}l$)	5×10^{-6} m	

Validation Tests against URL Permeability Measurements

Permeability Measurements in EDZs

Several large-scale underground experiments have been conducted at AECL's URL in Canada to address geomechanical issues related to the disposal of nuclear fuel waste. As part of these experiments, hydraulic characterization of EDZ was investigated in Room 425 of the TSX. The tunnel was excavated using the controlled drill and blast technique.

In situ hydraulic experiments, including pulse tests, were conducted around Room 425 at a depth of 425 m. The tests were performed using a SEPPI probe in eight short (3-4 m in length) radial boreholes drilled around Room 425. Typical variations of the in situ permeability in the roof and sidewalls of the tunnel are provided by Souley *et al.* (2001). The rock in the AECL's URL is predominantly Lac du Bonnet granite. Its mechanical properties have been extensively studied and well documented. The rock mass is basically intact, containing no or very few fractures. The in situ stresses in the AECL's URL are well understood. This site is an ideal site for the validation tests because of its simple geology and well-understood

rock properties and in situ stresses. Room 425 has an elliptical cross section. It is approximately 4.4 m along the longer axis and 3.5 m along the shorter axis. The tunnel is aligned to the maximum horizontal stress σ_1 , and its cross section is in the $\sigma_2 - \sigma_3$ plane.

Mechanical Input Parameters Used in the Validation Study

Rock mechanical parameters used for the validation study are mostly from the open literature for the AECL's URL, including Souley *et al.* (2001), Hajiabdomajid *et al.* (2002) and Martino and Chandler (2004). Some special input parameters needed for FRACOD modeling are not readily available from the literature. They have been assumed based on past experience. Where possible, sensitivity studies have been conducted to quantify the effect of the assumed parameters. The input parameters for the AECL's URL validation study are listed in Table 1.

FRACOD Models and Modeling Results

The numerical models include the elliptical opening of Room

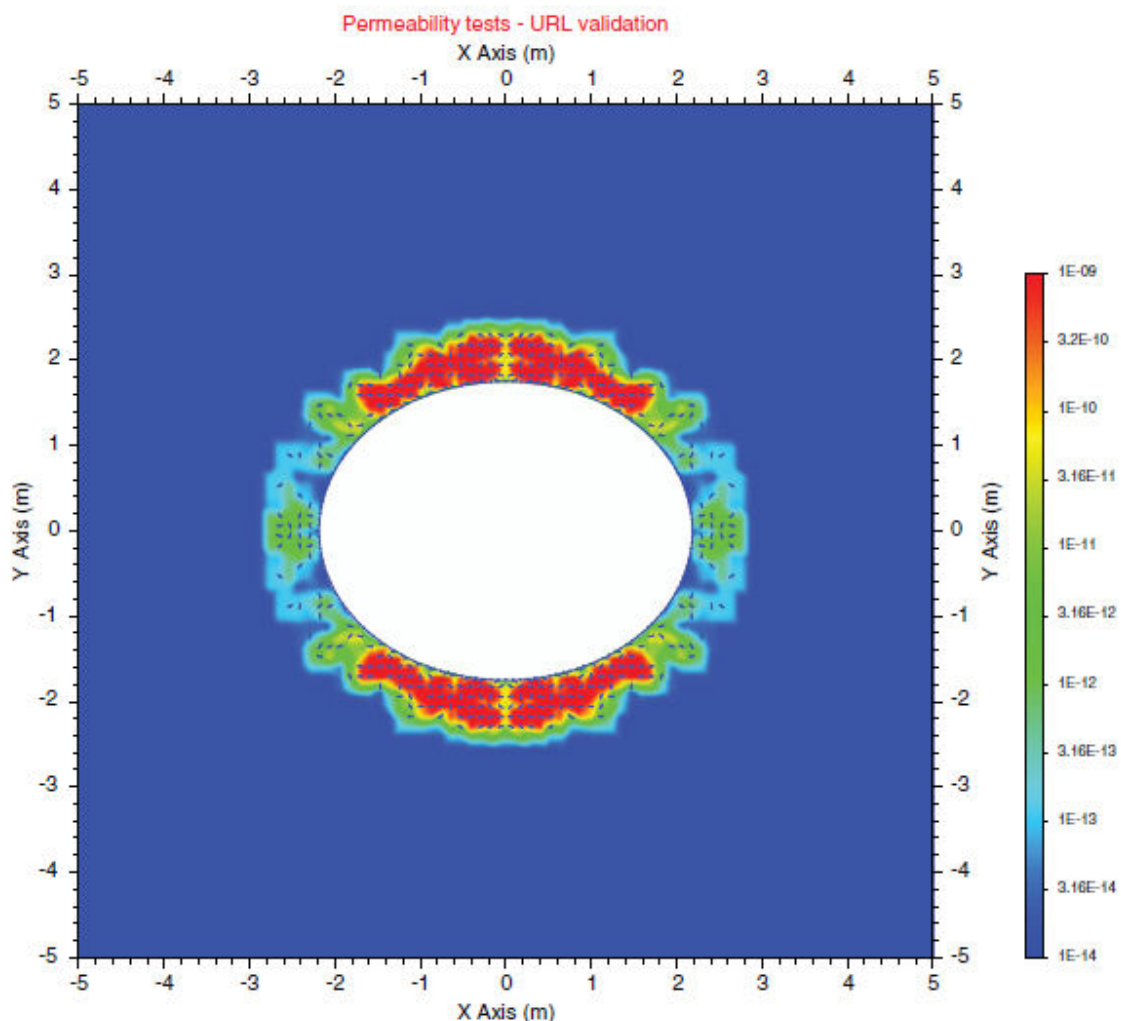


Figure 6. (Color) TDX experiment at URL, predicted EDZ and permeability K_x in Model 4; the intermediate principal stress (σ_2) is in the x -direction, whereas the minimum principal stress (σ_3) is in the y -direction

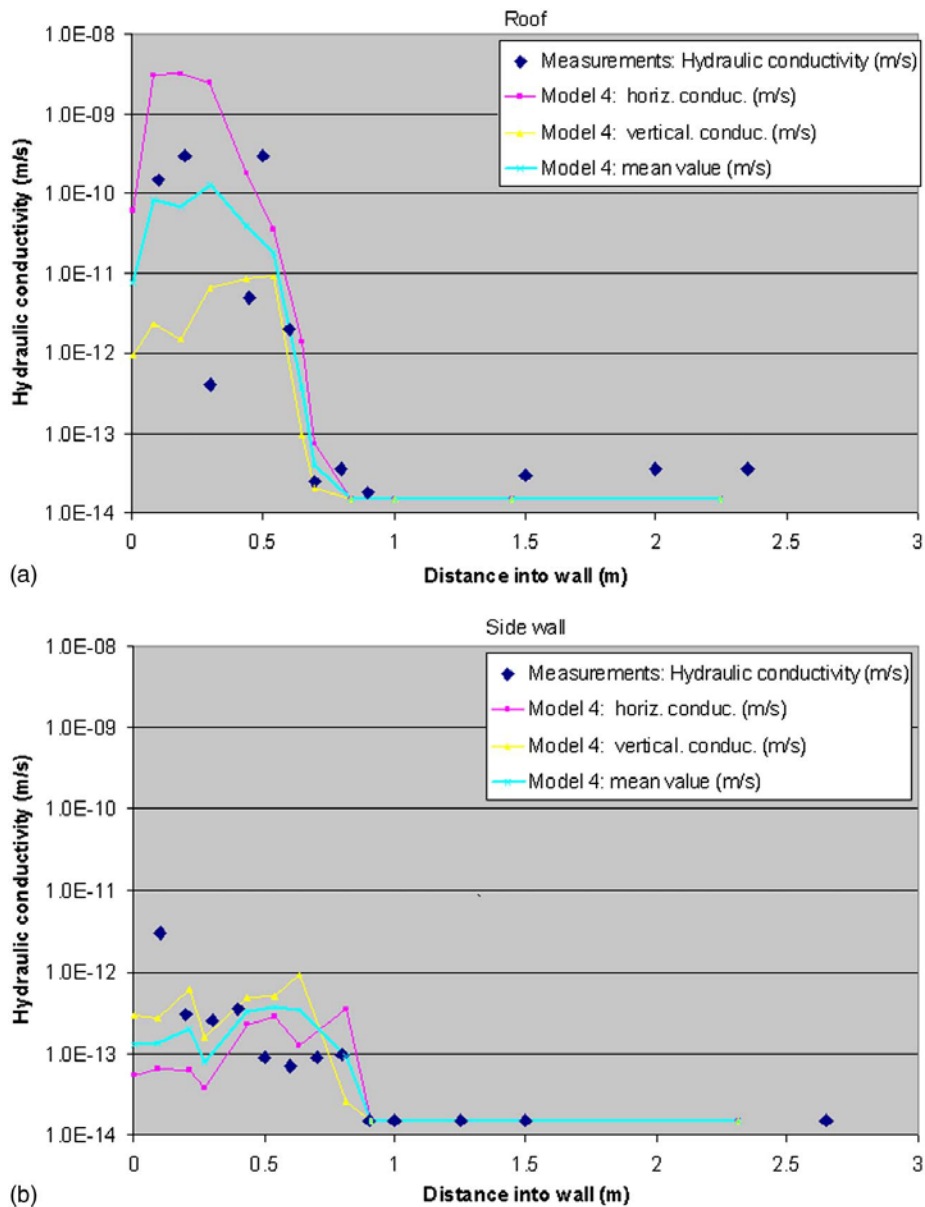


Figure 7. TDX experiment at URL, Model 4; measured and simulated hydraulic conductivity: (a) x -direction; (b) y -direction

425. The model's x - and y -axes are rotated to align with the intermediate and minor principal stresses. Four basic numerical models are used, which have different blast-damaged zone sizes. The blast damage is simulated by introducing randomly distributed short fractures within a specified distance from the excavation boundary.

- Model 1: No blast-induced fractures in rocks;
- Model 2: Random blast-induced fractures within 0.2 m into rocks;
- Model 3: Random blast-induced fractures within 0.4 m into rocks; and
- Model 4: Random blast-induced fractures within 0.6 m into rocks.

With or without the blast-induced fractures, all four models predict fracture initiations in the roof and floor of the elliptical cavern. The predicted EDZ and permeability of Model 4 are shown in Figs. 6 and 7. The zones of fracture initiation are approximately 0.5-0.7 m deep into the rock. The newly initiated fractures are not predicted to propagate under

the stress conditions applied. Therefore, no extensive spalling or breakout has been predicted to occur. This agrees with the observation at Room 425 that the excavation was generally stable. In the sidewalls of the elliptical cavern, no stress-induced fracture initiations are predicted because the stresses are released rather than increased from excavation. Any damage in these zones is likely to be caused by the excavation process rather than stress concentration.

The EDZs and the hydraulic conductivities in the roof and side-walls of the elliptical cavern using the four models were simulated. In each model, two hydraulic conductivity values are provided: one in the x -direction (subhorizontal), the other in the y -direction (subvertical). A geometrical mean value of the two values is also calculated. In the cavern roof, the predicted hydraulic conductivities of all four models agreed reasonably well with the measurement results [Fig. 7(a)]. The predicted EDZ is approximately 0.5-0.7 m from the excavation boundary. In the EDZ, the modeled hydraulic conductivity is mostly in the range of 1×10^{-12} to 1×10^{-9} m/s, which

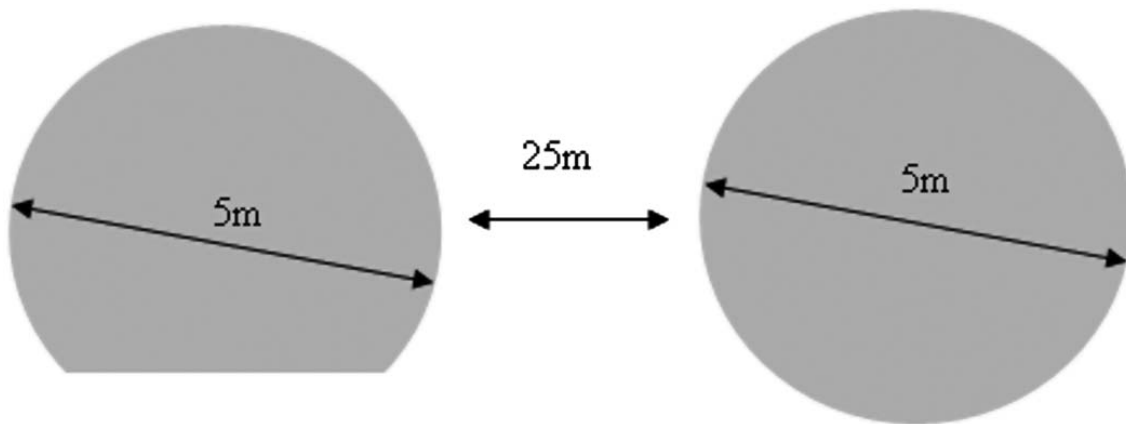


Figure 8. Geometry of the ZEDEX tunnels in Äspö Hard Rock Laboratory, Sweden

corresponds well with the measurement results.

In the sidewalls, Model 4 (with blast-induced cracks within 0.6 m into rock) produces the best results compared to the measurement results [Fig. 7(b)]. The modeled EDZ is approximately 0.7 m, and the hydraulic conductivity is approximately 1×10^{-13} to 1×10^{-12} m/s, and both are in general agreement with the measurements. Other models with no or smaller blast damage zones have predicted EDZs in the sidewalls smaller than the measurements, depending purely on the assumed extents of the blast damage. The stresses (tensile or compression) in these zones are not large enough to cause fracture initiation.

Because the horizontal stress is much higher than the vertical stress, the stress concentration at the cavern roof is high. This results in more rock damage in the roof than in the wall, and consequently the permeability is higher in the roof. In addition, new cracks in the roof are more likely to be generated in the horizontal direction (major principal stress direction). This will increase the horizontal permeability more than the vertical permeability.

Overall, the FRACOD modeling results agree well with

the permeability measurement data at Room 425, particularly in the cavern roof and floor. The numerical results also indicate that blast damage dominates the EDZs at the sidewalls but has little effect on the EDZs in the roof and floor where damage is caused by stress concentration. At AECL's URL, a blast damage assessment tunnel was excavated and investigated (Martino and Chandler 2004). It was found that the blast damage can extend up to 0.5 m into the walls. Therefore, the assumption of blast damage zone of 0.4-0.6 m in Models 3 and 4 is considered to be reasonable.

The predicted far-field permeability in the cavern roof does not match well with the measurements, but both values are very small. The measured results could be affected by limited measurement accuracy or local geological variation that the modeling did not consider.

Validation Tests against ZEDEX EDZ Measurements

ZEDEX was one of the first underground experiments conducted to study the damage and disturbance from excavation

Table 2. Input Parameters for the ZEDEX Validation Study

Input parameter	Value	Source
Rock type	Äspö diorite	Emsley et al. (1997)
Intact compressive strength (σ_c)	165 MPa	Rinne et al. (2003a)
Intact tensile strength (σ_t)	14.8 MPa	
Internal friction angle (ϕ)	49°	
Intact rock cohesion (c)	31 MPa	
Young's modulus (E)	68 GPa	
Poisson's ratio (ν)	0.24	
Fracture toughness: K_{Ic}	2.54 MPa m ^{1/2}	Rinne et al. (2003b)
Fracture toughness K_{IIc}	6.35 MPa m ^{1/2}	
In situ stresses σ_H (317.5°N)	-20.7 MPa	Chryssanthakis et al. (2003)
In situ stresses σ_v	-10.4 MPa	
In situ stresses σ_h	-9.6 MPa	
Fracture initiation level (σ_{ci})	0.3 σ_c and 0.12 σ_c	Emsley et al. (1997)
Fracture normal stiffness (K_n)	13,800 GPa/m	Assumed
Fracture normal stiffness (K_s)	3,099 GPa/m	
Fracture friction angle (ϕ)	49°	From intact rock strength
Fracture cohesion (c)	31 MPa	
Fracture dilation angle (ϕ_d)	5°	Assumed
In-situ hydraulic conductivity (K_{is})	1.5×10^{-13} m/s	Emsley et al. (1997)
Fracture initial aperture ($e_{initial}$)	10×10^{-6} m	Assumed
Fracture residual aperture (e_{resid})	5×10^{-6} m	

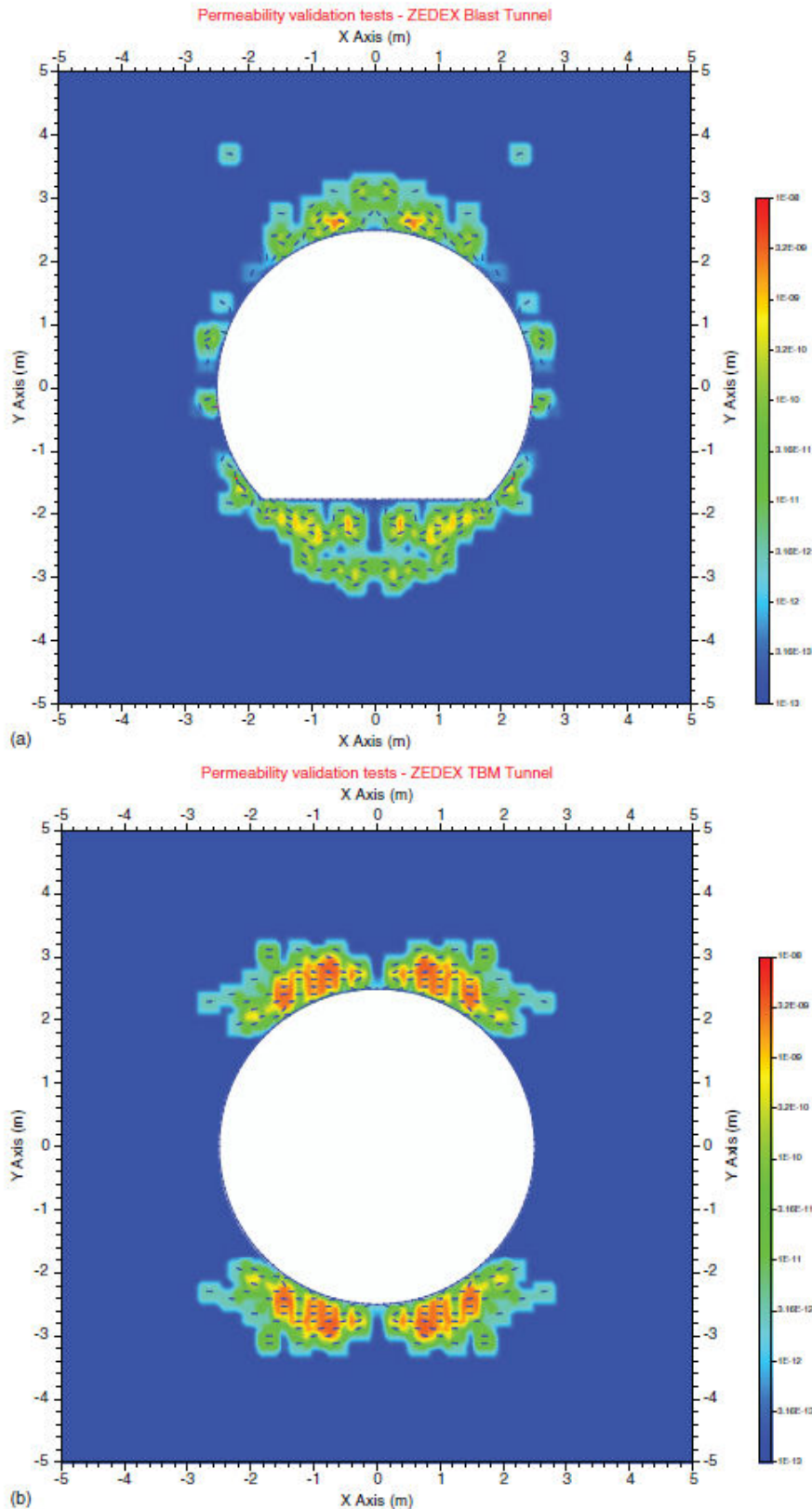


Figure 9. (Color) Predicted EDZ and hydraulic conductivity of (a) D&B tunnel; (b) TBM tunnel of the ZEDEX experiment at Äspö Hard Rock Laboratory, Sweden

by blasting and tunnel boring. It was conducted at ÄSPÖ Hard Rock Laboratory in Sweden at a depth of 420 m. Two parallel experimental tunnels were excavated, one by drill

and blast (D&B) and the other by TBM (Fig. 8). The D&B tunnel is a semicircular excavation with a flat floor. The TBM tunnel is a circular opening. Both tunnels have a diame-

Table 3. Input Parameters for the Tunnel at Crystalline Rock at Depth of 1,000 m

Input parameter	Value	Source
Rock type	Crystalline rock	Yamayama (personal communication)
Intact compressive strength (σ_c)	115 MPa	
Intact tensile strength (σ_t)	8 MPa	
Internal friction angle (ϕ)	45°	
Intact rock cohesion (c)	24 MPa	
Young's modulus (E)	37 GPa	
Poisson's ratio (ν)	0.25	
Fracture toughness K_{Ic}	1.73 MPa m ^{1/2}	Stephansson et al. (2003)
Fracture toughness K_{IIc}	3.07 MPa m ^{1/2}	
In situ stresses σ_H	-23.6 MPa	Yamayama (personal communication)
In situ stresses σ_v	-26.2 MPa	
Fracture initiation level (σ_{ci}):	0.3 σ_c	Emsley et al. (1997)
Fracture normal stiffness (K_n)	13,800 GPa/m	Stephansson et al. (2003)
Fracture normal stiffness (K_s)	3,099 GPa/m	
Fracture friction angle (ϕ)	45°	From intact rock strength
Fracture cohesion (c)	24 MPa	
Fracture dilation angle (ϕ_d)	2°	Stephansson et al. (2003)
In-situ hydraulic conductivity (K_{is})	1.0 × 10 ⁻⁹ m/s	Amemiya (personal communication)
Fracture initial aperture ($e_{initial}$)	10 × 10 ⁻⁶ m	Assumed
Fracture residual aperture ($e_{residual}$)	5 × 10 ⁻⁶ m	

ter of 5 m. The tunnels were driven in the direction of approximately 45° from the horizontal principal stresses.

Comprehensive tests were conducted to characterize the EDZs around the two tunnels (Emsley et al. 1997), including in situ stress measurements, AE monitoring, displacement monitoring, in situ and laboratory permeability tests, and seismic mapping. The results from ZEDEX indicate that the EDZ in the TBM tunnel is in the range of 0-0.35 m, depending upon the method of measurements. In the D&B tunnel, the EDZ is in the range of 0-1.5 m, and the deepest EDZ was measured in the floor.

Hydraulic conductivity was measured both in situ using pulse tests and in the laboratory using the oriented cores from drill holes. The in situ hydraulic conductivity is in the range of 1 × 10⁻¹¹ to 1 × 10⁻¹⁰ m/s, is highly irregular, and is possibly affected by the preexisting fractures. The laboratory measurements indicate that in the TBM tunnel walls, the hydraulic conductivity falls within a narrow range from 1 × 10⁻¹³ to 6 × 10⁻¹³ m/s, whereas in the D&B tunnel, it ranges from 1 × 10⁻¹³ to 6 × 10⁻⁹ m/s. In both tunnels, an obvious increase of hydraulic conductivity was measured within 0.2-0.6 m into the tunnel walls.

The ZEDEX experiments are a complicated case for the code validation tests, primarily because (1) the geology is complex and fractures are well developed at the ZEDEX site; (2) the in situ stresses are not fully understood - uncertainties exist in the measured and extrapolated stresses at the ZEDEX site; and (3) the EDZs are very limited, making it difficult to study the stress-induced fractures. Therefore, this study of the ZEDEX experiment is more qualitative than quantitative.

Input Parameters

Rock mechanical parameters used for the validation study at the ZEDEX site are primarily based on the SKB technical report by Emsley et al. (1997), Chrystanthakis et al. (2003), and Rinne et al. (2003b). The input parameters for the

ZEDEX validation study are listed in Table 2.

Two fracture initiation levels (0.3 σ_c and 0.12 σ_c) are used in this study. The first is based on the previous laboratory tests and the AECL results, whereas the second is based the AE monitoring at ZEDEX experiments (Emsley et al. 1997). It has been argued by Emsley et al. (1997) whether the measured AEs at ZEDEX represent the fracture initiation because it is significantly lower than the normal level. It could be also possible that the actual in situ stresses are higher than measured, resulting in a higher fracture initiation level than 0.12 σ_c . Results from fracture initiation stress 0.12 σ_c are presented in this contribution.

FRACOD Models and Modeling Results

The D&B tunnel and the TBM tunnel are simulated separately using two models, each assumed to be in an infinite rock mass. The following four cases were studied:

- Case D&B1: D&B tunnel without blast-induced fractures;
- Case D&B2: D&B tunnel with blast-induced fractures;
- Case TBM1: TBM tunnel without blast-induced fractures; and
- Case TBM2: TBM tunnel with fractures corresponding to blast-induced fractures.

The modeling results for tunnels with fracture initiation level 0.12 σ_c are shown in Fig. 9. The predicted EDZ is predominately in the roof and floor of the tunnels where stress concentration occurs because of the higher horizontal stress than the vertical stress. For the D&B tunnel, the EDZ extends up to 1.3 m into the floor and 0.8 m into the roof, but very limited distance into the sidewalls. For the TBM tunnel, the EDZ extends approximately 0.7 m into both the roof and floor and an insignificant distance into the sidewalls.

The predicted hydraulic conductivity in the EDZ ranges from the background value of 1 × 10⁻¹³ m/s to a maximum value of approximately 1 × 10⁻⁹ m/s. The maximum value agrees well with the measured hydraulic conductivity in the

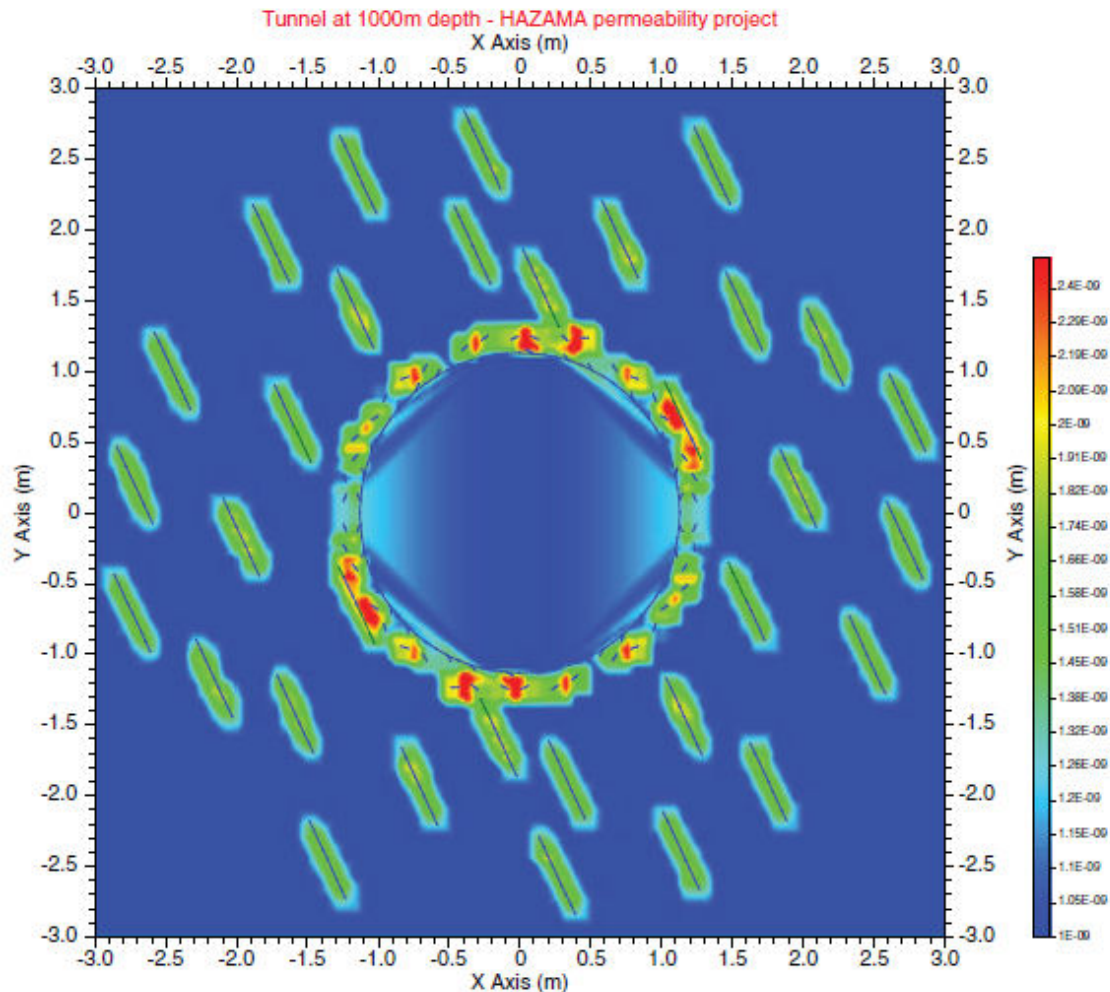


Figure 10. (Color) FRACOD simulation of EDZ and hydraulic conductivity in a tunnel of fractured hard rocks at a depth of 1,000 m for the Japanese radioactive waste program

vertical boreholes of the D&B tunnel, which is approximately 1×10^{-9} m/s [or 1×10^{-16} m² in the report by *Emsley et al.* (1997)]. However, the predicted hydraulic conductivity does not agree with the very low values measured in the roof and floor of the TBM tunnel.

The FRACOD models also predict a maximum convergence of 2.6 mm in the D&B tunnel and 2.8 mm in the TBM tunnel. The measured maximum convergence at two locations of the TBM tunnel is 3.6 mm and 1.3 mm, respectively. Their average value of 2.5 mm agrees well with the FRACOD model predictions.

Overall, the predicted EDZs in the ZEDEX tunnels are in a broad agreement with the measurements, taking into account the uncertainties in the in situ stresses and the local fracture initiation levels.

FRACOD Prediction of EDZ Permeability for Deposition Tunnels in Japan

FRACOD is applied to predict the EDZ and the permeability change around a deposition tunnel for the Japanese concept of radioactive waste disposal in hard rocks. The repository

consists of parallel deposition tunnels with a diameter of 2.26 m. The distance between tunnels is six times the tunnel diameter. Input parameters used in the FRACOD models for crystalline rock at depth of 1,000 m are shown in Table 3.

The existence of preexisting fractures has some effect on the EDZ (Fig. 10). The preexisting fractures within 0.5 m from the tunnel wall are partially activated and experiencing shear slipping. The slipping fractures, however, are not predicted to propagate, and the tunnel remains stable. The maximum hydraulic conductivity in the EDZ is approximately 5.0×10^{-9} , which occurs at the preexisting fractures near the tunnel.

Conclusions

A systematic study is conducted in this contribution to investigate the feasibility of using FRACOD to predict the EDZ and permeability change for nuclear waste disposal. This study includes

- Detailed formulations to estimate the hydraulic conductivity of an explicitly fractured rock mass. The calculated hydraulic conductivity allows inflow calculations to be

made once the hydraulic boundary conditions and rock mass properties are known.

- Theoretical formulations implemented into FRACOD, and the new code version can now predict the rock mass hydraulic conductivity during rock fracture initiation, propagation, and coalescence.
- Validation tests of FRACOD conducted against AECL's URL permeability measurement results in the TSX tunnel. The FRACOD model predicts the EDZ and its permeability that are consistent with the measurement data, particularly in the roof/floor region of the TSX tunnel where stress concentrations exist. In the sidewalls where stress release occurs, the model has to include the blast-induced fractures to produce results reasonably close to the measurements.
- Validation tests carried out against the ZEDEX measurement results in the Drill and Blast Tunnel and the TBM Tunnel at Äspö Hard Rock Laboratory. An overall agreement between the FRACOD prediction and measurements has been achieved. The uncertainties in in situ stress data and the fractures at the ZEDEX site, however, made it difficult for a detailed comparison between the numerical results and measurements.

The validation tests against both the AECL URL measurements and the ZEDEX measurements indicate that FRACOD is capable of realistically predicting the EDZ and permeability change. In addition, the tests also provide confidence on the input parameters used in the FRACOD models.

Following the validation tests, FRACOD is applied to study the EDZ of the conceptual deposition tunnels for radioactive waste in Japan. When the tunnels are excavated at depth of 1,000 m in a crystalline fractured rock, the predicted EDZ is limited within 0.25 m into the tunnel walls, and the hydraulic conductivity in the EDZ is less than 5.0×10^{-9} m/s. The limited EDZ is attributable to the nearly hydrostatic stress condition and high rock strength.

Acknowledgments

The development of the permeability function in FRACOD and the conduction of validation tests were kindly supported by the Hazama Corporation, Japan.

References

Chryssanthakis, P., Tunbridge, L., and Christiansson, R. (2003). "Numerical modelling in 3D of the TBM/ZEDEX tunnels at Äspö, Hard Rock Laboratory and comparison

with in-situ measurements." *Proc., Underground Construction Conference*, London.

- Emsley, S., Olsson, O., Stenberg, L., Alheid H.-J., and Falls, S. (1997). "Zedex - A study of damage and disturbance from tunnel excavation by blasting and tunnel boring." *SKB Technical Rep. 97-30*, Swedish Nuclear Fuel and Waste Management Co., Stockholm, Sweden.
- Hajiabdolmajid, V., Kaiser, P. K., and Martin, C. D. (2002). "Modelling brittle failure of rock." *Int. J. Rock Mech. Min. Sci.*, 39(6), 731-741.
- Martino, J. B., and Chandler, N. A. (2004). "Excavation-induced damage studies at the Underground Research Laboratory." *Int. J. Rock Mech. Min. Sci.*, 41(8), 1413-1426.
- Rinne, M., Shen, B., and Lee, H.-S. (2003a). "Äspö Hard Rock Laboratory". Äspö pillar stability experiment. Modelling of fracture stability by FRACOD. Preliminary results." *SKB IPR-03-05*, Swedish Nuclear Fuel and Waste Management Co., Stockholm, Sweden.
- Rinne, M., Shen, B., Lee, H.-S., and Jing, L. (2003b). "Thermo-mechanical simulations of pillar spalling in SKB APSE test by FRACOD." *Geo-Proc2003, Int. Workshop*, Stockholm.
- Shen, B. (2002). *FRACOD Version 1.1 user's manual*, FRACOM Ltd., Kyrkslätt, Finland.
- Shen, B. (2004). "Development of FRACOD for multiple region problems." *FRACOM Ltd. Rep. (2004) Prepared for Hazama Corporation*, FRACOM Ltd., Kyrkslätt, Finland.
- Shen, B., Rinne, M., and Stephansson, O. (2006). "Development of FRACOD for permeability modelling in MIU Project." *FRACOM Rep. Prepared for Hazama Corporation*, FRACOM Ltd., Kyrkslätt, Finland.
- Shen, B., and Stephansson, O. (1994). "Modification of the G-criterion for crack propagation subjected to compression." *Eng. Fract. Mech.*, 47(2), 177-189.
- Shen, B., Stephansson, O., and Rinne, M. (2002). "Simulation of borehole breakouts using FRACOD^{2D}." *Oil Gas Sci. Technol.*, 57(5), 579-590.
- Souley, M., Homand, F., Pepa, S., and Hoxha, R. (2001). "Damage-induced permeability changes in granite: A case example at the URL in Canada." *Int. J. Rock Mech. Min. Sci.*, 38(2), 297-310.
- Stephansson, O., et al. (2003). "Mechanical evaluation and analysis of research shafts and galleries in MIU Project, Japan (Paper No. UE03-K9)." *1st UE Kyoto Symp.*, Kyoto, Japan.
- Tsang, C.-F., Bernier, F., and Davies, C. (2005). "Geohydro-mechanical processes in the excavation damaged zone in crystalline rock, rock salt and indurated and plastic clays - In the context of radioactive waste disposal." *Int. J. Rock Mech. Min. Sci.*, 42(1), 109-125.